

Shape anisotropy effect on magnetization reversal induced by linear down chirp pulse

Z. K. Juthy^a, M. A. J. Pikul^a, M. A. S. Akanda^a and M. T. Islam^{a,*}

^aPhysics Discipline, Khulna University, Khulna 9208, Bangladesh

ARTICLE INFO

Keywords:

Magnetization reversal
Shape anisotropy
Energy barrier
Stimulated energy absorption/emission

ABSTRACT

We investigate the influence of shape anisotropy on the magnetization reversal of a single-domain magnetic nanoparticle driven by a circularly polarized linear down-chirp microwave field pulse (DCMP). Based on the Landau-Lifshitz-Gilbert equation, numerical results show that the three controlling parameters of DCMP, namely, microwave amplitude, initial frequency and chirp rate, decrease with the increase of shape anisotropy. For certain shape anisotropy, the reversal time significantly reduces. These findings are related to the competition of shape anisotropy and uniaxial magnetocrystalline anisotropy and thus to the height of energy barrier which separates the two stable states. The result of damping dependence of magnetization reversal indicates that for a certain sample shape, there exists an optimal damping situation at which magnetization is fastest. Moreover, it is also shown that the required microwave field amplitude can be lowered by applying the spin-polarized current simultaneously. The usage of an optimum combination of both microwave field pulse and current is suggested to achieve cost efficiency and faster switching. So these findings may provide the knowledge to fabricate the shape of a single domain nanoparticle for the fast and power-efficient magnetic data storage device.

1. Introduction

Obtaining fast and energy-efficient magnetization reversal of single-domain of the perpendicularly magnetized nanoparticle is an interesting issue owing to its potential application in high-density data storage devices [1, 2, 3] and rapid data access [4]. For high density, high thermal stability and low error rate in device application, high anisotropy materials [5] are needed. But it is a challenge to find out a way with low energy to achieve the fastest magnetization reversal for high-anisotropy magnetic nanoparticle. Over the past two decades, several controlling parameters/driving forces are discovered to achieve fastest magnetization reversal with low cost. Namely, magnetization reversal using a constant magnetic field [6, 7], reversal by microwave field of constant frequency or time dependent frequency, either with or without a polarized electric current [8, 9, 10, 11, 12, 13, 14, 15, 16, 17, 18, 19] and by spin transfer torque (STT) or spin orbit torque (SOT) [20, 21, 22, 23, 24, 25, 26, 27, 28, 29, 30, 31, 32, 33, 34]. All methods mentioned above are suffering from specific drawbacks [6, 35, 36, 37, 38, 39, 40, 41]. For example, magnetic field or microwave field driven magnetization is not energy efficient and fast as expected. In case of current (by STT) or SOT driven, the higher threshold current requirement is a bottleneck. Later on, researchers are digressed to employ the microwave chirped pulses (microwave with time-dependent frequency) which induce fast and energy-efficient magnetization reversal [13, 14, 15, 16, 17, 19] but still the required field amplitude, initial frequency and chirp rate are not small as desired prac-

tically. Recent studies [42, 43] have demonstrated that the fast magnetization reversal of a cubic nanoparticle (i.e., with zero demagnetization/shape anisotropy) obtained by the linear down chirp microwave pulse (DCMP). The physical mechanism of this model is that the DCMP (whose frequency linearly decreases from initial $+f_0$ to final $-f_0$) stimulates microwave energy absorption (emission) by the magnetic moment before (after) crossing the energy barrier. The efficiency of the microwave energy absorption/emission depends on how closely the microwave frequency and magnetization intrinsic frequency match during reversal. This frequency-matching is related to the energy barrier [44, 45]. However, in small-scale nanoparticle, demagnetization field/shape anisotropy (which was excluded previously) has a great importance [46, 47, 44] because, it interacts/opposes the dominated uniaxial magnetocrystalline anisotropy and thus reduces the energy barrier between two stable states. So, the magnetization reversal of a nanoparticle with finite shape anisotropy might be faster and energy efficient. In addition, fabricating perfect cubic nanoparticle (i.e., with zero demagnetization field) is a challenging issue from practical point of view. For the most device applications, the desired microwave pulse (DCMP) should be with smaller amplitude, initial frequency and low chirp rate.

Therefore, this study focuses on how the shape anisotropy H_{shape} affects the energy consumption i.e., the amplitude H_{mw} , initial frequency f_0 and pulse chirp rate η of DCMP and the magnetization switching time t_s . Interestingly, we found that the parameters of DCMP i.e., H_{mw} , f_0 , and η decrease with the increase of shape anisotropy H_{shape} . In addition, there is a critical H_{shape} or cross-sectional area A , for which or larger, t_s significantly reduces to 0.346 ns which is close to the theoretical limit [40]. For instance, in case of a sample of cross-sectional area $32 \times 32 \text{ nm}^2$, or $H_{\text{shape}} = 0.598 \text{ T}$, we estimated $t_s = 0.346 \text{ ns}$, $H_{\text{mw}} = 0.0187 \text{ T}$,

*Corresponding authors:

✉ torikul@phy.ku.ac.bd (M.T. Islam)

ORCID(s): 0000-0002-4168-8695 (Z.K. Juthy); 0000-0002-7500-1572

(M.A.J. Pikul); 0000-0002-6742-2158 (M.A.S. Akanda);

0000-0002-3846-4009 (M.T. Islam)

$f_o = 5.2$ GHz, and optimal $\eta = 24.96$ ns⁻² which are significantly smaller than $t_s = 0.56$ ns, $H_{mw} = 0.045$ T, $f_o = 21$ GHz, and optimal $\eta = 67.2$ ns⁻² for the cubic shaped or zero H_{shape} . The physical reason of these findings is related to the competition between shape anisotropy and the uniaxial magnetocrystalline anisotropy. The findings of damping dependence of magnetization reversal indicate that, for a specific A or H_{shape} , there exists a optimal damping situation. Moreover, this study shows that the required microwave field amplitude of DCMP can be lowered by applying direct current simultaneously along with DCMP. Therefore, an optimum combination of microwave field pulse and current could be applied to achieve faster and power efficient magnetization reversal. So these findings might be significant to design the shape of single domain nanoparticle to produce the low-energy cost magnetic storage device with high speed data processing.

2. Analytical Model and Method

We consider a spin valve system that consists of a free and fixed ferromagnetic layers by sandwiching a nonmagnetic spacer, as shown schematically in Figure 1(a). The free layer is a square nanoparticle of area A and thickness d . The magnetization direction of the fixed and free layer is along \hat{z} direction, i.e., both are perpendicularly magnetized. The magnetization of the free layer can be treated as a macrospin represented by the unit moment \mathbf{m} with total magnetization AdM_s , where M_s represents the saturation magnetization. The demagnetization field, which generated by the magnetization of nanoparticle, can be approximated by an easy-plane shape anisotropy. The demagnetization field/shape anisotropy field is expressed as $\mathbf{H}_{shape} = H_{shape}m_z\hat{z}$ such that $H_{shape} = -\mu_0(N_z - N_x)M_s$, is the shape anisotropy coefficient, where N_z and N_x are demagnetization factors [45] and $\mu_0 = 4\pi \times 10^{-7}$ N/A² is the vacuum magnetic permeability. Because of the strong uniaxial magnetocrystalline anisotropy $\mathbf{H}_{ani} = H_{ani}m_z\hat{z}$, the magnetization of the free layer prefers to stay in two ground states, i.e., \mathbf{m} parallel to \hat{z} and $-\hat{z}$.

Under the circularly polarized DCMP and spin polarized current, the magnetization dynamics \mathbf{m} is governed by the Landau-Lifshitz-Gilbert (LLG) equation [7, 9, 37, 48]

$$\frac{d\mathbf{m}}{dt} = -\gamma\mathbf{m} \times \mathbf{H}_{eff} + \alpha\mathbf{m} \times \frac{d\mathbf{m}}{dt} - \gamma h_s\mathbf{m} \times (\mathbf{p} \times \mathbf{m}) \quad (1)$$

where α is the dimensionless Gilbert damping constant and, γ is gyromagnetic ratio. \mathbf{H}_{eff} is the total effective field which contains the microwave magnetic field \mathbf{H}_{mw} , the exchange field $\frac{2A}{M_s}\nabla^2\mathbf{m}$ where A is the exchange stiffness constant, and the effective anisotropy field \mathbf{H}_k along z direction, i.e., $\mathbf{H}_k = H_k m_z \hat{z}$. h_s is the strength of spin transfer torque (STT),

$$h_s = \frac{\hbar PJ}{2e\mu_0 M_s d} \quad (2)$$

where J , e , \hbar , P , μ_0 and d denote the current density, electron charge, the Planck's constant, spin polarization of cur-

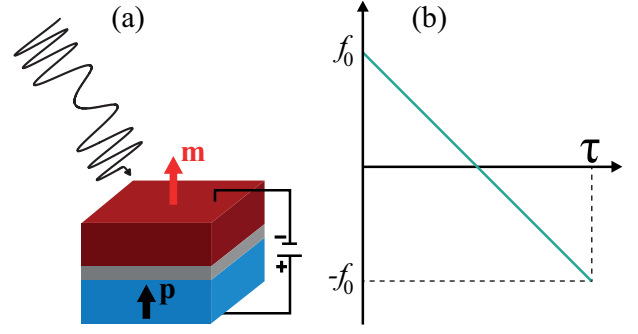


Figure 1: (a) Schematic diagram of the system in where \mathbf{m} and \mathbf{p} denote the unit vectors of the magnetization of free layer and fixed layer, respectively. A linear down-chirp microwave field and an electric current are applied on a single domain nanoparticle. (b) The frequency profile illustrates (sweeping from $+f_0$ to $-f_0$) the linear down-chirp microwave field.

rent, the vacuum permeability, and thickness of the free layer, respectively.

The \mathbf{H}_k has two components: an uniaxial magnetocrystalline anisotropy \mathbf{H}_{ani} and a shape anisotropy \mathbf{H}_{shape} field which can be expressed as $\mathbf{H}_k = \mathbf{H}_{ani} + \mathbf{H}_{shape} = [H_{ani} - \mu_0(N_z - N_x)M_s]m_z\hat{z}$. Thus, the resonant frequency of the nanoparticle can be found from the Kittel formula $f_0 = \frac{\gamma}{2\pi}[H_{ani} - \mu_0(N_z - N_x)M_s]$.

We first apply only the microwave field-driven magnetization reversal, i.e., without electric current (SST) term, the rate of energy change is expressed as

$$\dot{e} = -\alpha\gamma |\mathbf{m} \times \mathbf{H}_{eff}|^2 - \mathbf{m} \cdot \dot{\mathbf{H}}_{mw} \quad (3)$$

Since damping is positive, so, the first term is always negative. For time-dependent external microwave field, depending on the angle between the instantaneous magnetization \mathbf{m} and $\dot{\mathbf{H}}_{mw}$, the second term can be either positive or negative, in other words, the microwave field pulse can trigger stimulated energy absorption or emission.

It has been shown that the fast magnetization reversal is achieved by DCMP [42] with the physical picture: the frequency of DCMP matches the frequency change of magnetization precession. Hence, it triggers stimulated microwave absorption (emission) by (from) the magnetization before (after) it crosses over the energy barrier.

The microwave field that we have applied takes the form,

$$\mathbf{H}_{mw} = H_{mw} [\cos \phi(t)\hat{x} + \sin \phi(t)\hat{y}] \quad (4)$$

where H_{mw} is the amplitude of the microwave field and $\phi(t)$ is the phase. In this paper, we use a DCMP whose instantaneous frequency is defined as $f(t) = \frac{1}{2\pi} \frac{d\phi}{dt}$, which linearly decreases with time at constant rate η (in units of ns⁻²) as shown in Figure 1(b). The phase $\phi(t)$ and the instantaneous frequency $f(t)$ are given by,

$$\phi(t) = 2\pi(f_0 t - \frac{\eta}{2} t^2); \quad f(t) = f_0 - \eta t \quad (5)$$

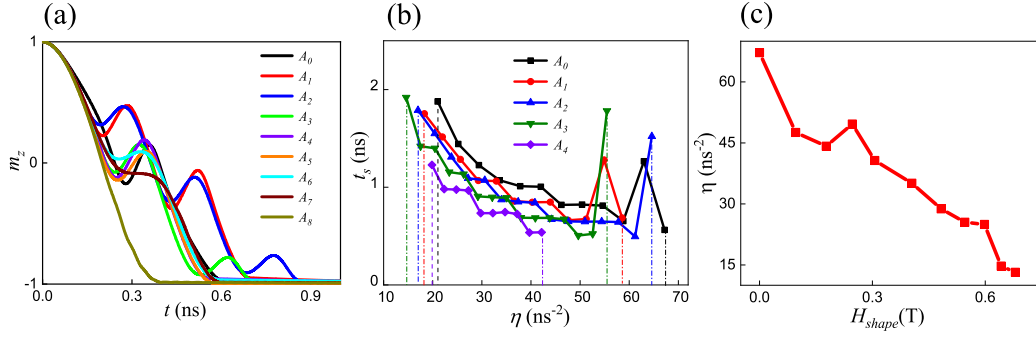


Figure 2: Model parameters of the free layer, $M_s = 10^6$ A/m, $A_{\text{ex}} = 13 \times 10^{-12}$ J/m, $H_k = 0.75$ T, $\gamma = 1.76 \times 10^{11}$ rad/(T·s), and $\alpha = 0.01$. (a) Temporal evolution of m_z induced by DCMP with $H_{\text{mw}} = 0.045$ T for the samples of different A . (b) The dependence of switching time t_s on the chirp rate η for different cross-sectional areas while keeping the microwave field amplitudes H_{mw} constant. The vertical dashed lines indicate the lower and upper limits of η for magnetization switching. (c) The dependence of chirp rate η on shape anisotropy H_{shape} for switching time within 1 ns.

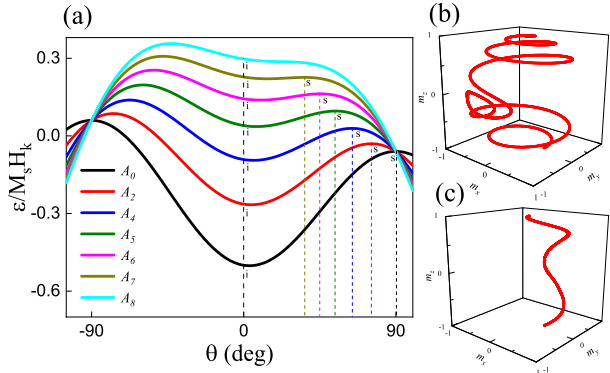


Figure 3: (a) The potential ϵ along the line $\phi = 0$ for the samples of different A . Angles θ and ϕ are defined as $\cos^{-1} m_z$ and $\tan^{-1}(m_x/m_y)$. The symbols i and s represent the initial state and the saddle point, respectively. Magnetization reversal trajectories of (b) $A_0 = 8 \times 8$ nm² and (c) $A_8 = 32 \times 32$ nm².

where f_0 is the initial frequency at $t = 0$. The duration of the microwave pulse is $\tau = \frac{2f_0}{\eta}$ which means the final frequency is $-f_0$. According to the applied DCMP, the second term of Eq. (3) can be expressed as

$$\dot{\epsilon} = -H_{\text{mw}} \sin \theta(t) \sin \Phi(t) \frac{d\Phi}{dt} \quad (6)$$

where $\Phi(t)$ is the angle between \mathbf{m}_t (the in-plane component of \mathbf{m} and \mathbf{H}_{mw}). Therefore, the microwave field pulse can trigger the stimulated energy absorption (for $-\Phi(t)$) which is occurred before crossing the energy barrier and emission (for $\Phi(t)$) after crossing the energy barrier.

For this study, the parameters of Permalloy are chosen from typical experiments on microwave-driven magnetization reversal as $M_s = 10^6$ A/m, $H_{\text{ani}} = 0.75$ T, $\gamma = 1.76 \times 10^{11}$ rad/(T·s), $A_{\text{ex}} = 13 \times 10^{-12}$ J/m and $\alpha = 0.01$. Although, the demonstrated strategy and findings would still be valid for other materials. The cell size used throughout this study is $(2 \times 2 \times 2)$ nm³. We solved the LLG equa-

tion numerically using the MUMAX3 package [49] for time-dependent circularly polarized microwave field. We consider the switching time window of 1 ns and least magnetization reversal $m_z = -0.9$.

3. Numerical Results

In a small-scale nanoparticle, demagnetization field or shape anisotropy field H_{shape} is an important property to take into account in the investigation of the magnetization reversal. In order to approximate demagnetization field/shape anisotropy H_{shape} , we choose cuboid shaped sample/nanoparticle of volume $V = Ad$, where A is the cross-sectional area and d is the height. To increase the demagnetization field strength or H_{shape} , A is gradually increased while the thickness $d = 8$ nm is kept fixed. Specifically, we intend to investigate the magnetization reversal of the samples, $A_1 = 10 \times 10$, $A_2 = 12 \times 12$, $A_3 = 14 \times 14$, $A_4 = 16 \times 16$, $A_5 = 20 \times 20$, $A_6 = 24 \times 24$, $A_7 = 28 \times 28$, $A_8 = 32 \times 32$ nm². For each sample, by finding the demagnetization factors [45] N_z and N_x , the shape anisotropy coefficient $H_{\text{shape}} = \mu_0(N_z - N_x)M_s$ are calculated analytically. $\mathbf{H}_{\text{shape}}$ actually acts along $-z$ i.e., it opposes the intrinsic easy axis anisotropy field \mathbf{H}_{ani} and hence reduces the effective anisotropy. Therefore, for each A , the resonance/theoretical frequency is estimated by well-known Kittel-formula $f_0 = \frac{\gamma}{2\pi} [H_{\text{ani}} - \mu_0(N_z - N_x)M_s]$ as shown in the Table 1.

To investigate the DCMP-driven magnetization reversals of nanoparticles of different A , by keeping $H_{\text{mw}} = 0.045$ T and f_0 (close to resonant frequency corresponding to A or H_{shape}) fixed, we estimate the optimal η for each sample or H_{shape} . Figure 2(b) shows the η dependence of t_s for several samples or H_{shape} . It is noted that there exists a window of η denoted by vertical dashed line. For a small range of η in the right edge of window, the t_s is minimal. It means that there is a flexible space to choose η . In addition, the optimal $\eta(H_{\text{shape}})$ decreases with H_{shape} as shown in the Figure 2(c). These findings are useful in device application since it was reported that generating DCMP with higher chirp rate is a

Table 1

 Simulated values of the controlling parameters for different samples of cross-sectional area A

Cross-sectional area A (nm ²)	Shape anisotropy field h_{shape} (T)	Natural frequency f_0 (GHz)	Simulated minimal frequency f_0 (GHz)
A_1	0.09606	18.3	18.3
A_2	0.17718	16	17
A_3	0.2465	14.1	14.
A_4	0.3064	12.4	12.4
A_5	0.4049	9.6	10.2
A_6	0.4827	7.49	9
A_7	0.5457	5.72	7.5
A_8	0.5980	4.26	5.2

challenge [42]. Afterward, DCMP (with $H_{\text{mw}} = 0.045$, f_0 corresponding to H_{shape} and optimal $\eta(H_{\text{shape}})$) driven magnetization reversals are investigate and thus the time evolutions of m_z for different H_{shape} or A are shown in the Figure 2(a). It is found that with the increase of H_{shape} , the magnetization switching time t_s remains almost same until $A_7 = 28 \times 28 \text{ nm}^2$ but for $A_8 \geq 32 \times 32 \text{ nm}^2$, the magnetization reverses very smoothly i.e., t_s drops to $= 0.34 \text{ ns}$ which is close to the theoretical limit (0.39 ns) [40]. So, it is mentioned that there is a critical A and for larger values than it, the switching time becomes significantly smaller which is an ultimate demand in device application.

To understand the reason why fast reversal is obtained, one can recall that the energy barrier is proportional to the effective anisotropy field [39, 40]. Since the H_{shape} opposes the anisotropy field H_{ani} and thus reduces the height of the energy barrier (energy difference between the initial state and saddle point). This reduction of energy barrier for different A is presented in the Figure 3(a). Therefore, the magnetization reversal becomes easier and faster because the microwave frequency and magnetization precession frequency closely matches as expected. To be more explicit, one may look at the trajectories of magnetization reversal for two cases of A or H_{shape} in Figure 3(b) and 3(c). For $A_0 = 8 \times 8 \text{ nm}^2$ or $H_{\text{shape}} = 0$, the magnetization takes a longer time because of some additional precessions while crossing the higher energy barrier. However, for $A_8 = 32 \times 32 \text{ nm}^2$ or $H_{\text{shape}} = 0.598 \text{ T}$, the magnetization reversal is fairly smooth i.e., without any additional precessions since the energy barrier is reduced by H_{shape} . For more justification, Fig 4 (a) shows the change the angle Φ (blue) and m_z (black line) with time for $A_8 = 32 \times 32 \text{ nm}^2$. Note that the angle Φ remains almost 90° during magnetization reversal which is desired for triggering an efficient microwave energy absorption (emission) by magnetization. Thus the corresponding energy changing rate $\dot{\epsilon}$ (red), in Fig 4(c) is obtained with absorption and emission peaks (no distortion) which lead fast reversal. However, Fig 4(b), for $A_0 = 8 \times 8 \text{ nm}^2$ i.e., for zero H_{shape} , shows the $\dot{\epsilon}$ (red line) absorption and emission peaks (distorted) indicating inefficient i.e., slower magnetization reversal (black line).

Then, for the DCMP with fixed $H_{\text{mw}} = 0.045 \text{ T}$ and optimal chirp rate $\eta(H_{\text{shape}})$, we obtain the fast magnetization

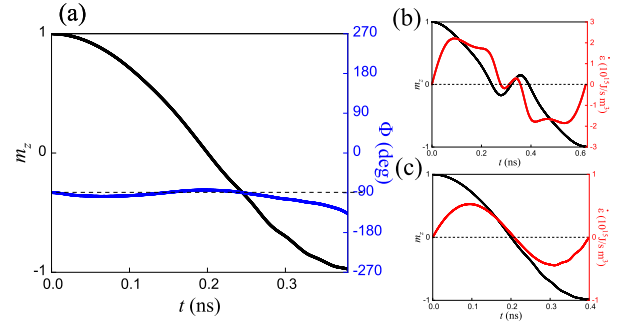


Figure 4: (a) For $A_8 = 32 \times 32 \text{ nm}^2$, the plot of the relative angle Φ against time (blue line) and the time dependence of m_z (black line). Plots of the energy changing rate $\dot{\epsilon}$ of magnetization against time (red line) and the time dependence of m_z (black line) for the cross-sectional area (b) $A_0 = 8 \times 8 \text{ nm}^2$ and (c) $A_8 = 32 \times 32 \text{ nm}^2$

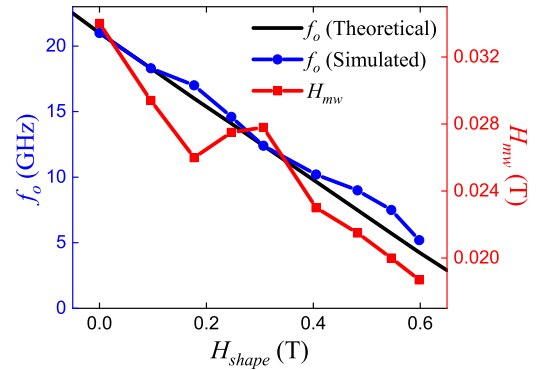


Figure 5: The dependence of initial frequency f_0 and minimum required field amplitude H_{mw} as a function of shape anisotropy H_{shape} for switching time within 1 ns.

reversal of different A for a certain range of f_0 around each resonance/natural frequency. There exist a minimal f_0 , i.e., minimal f_0 corresponding to each sample, for which switching time is lowest. Figure 5 shows the simulated minimal frequency f_0 (blue circles) as a function of H_{shape} and found that the simulated f_0 (blue circles) of DCMP decreases with increasing H_{shape} . These can be explained as the H_{shape} reduces the effective anisotropy H_k . For further justification,

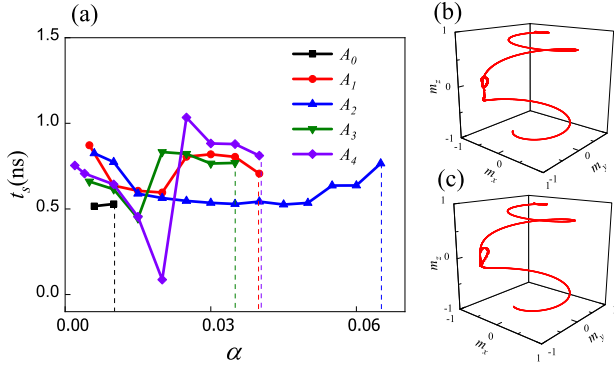


Figure 6: (a) Minimal switching time for the samples of different A as a function of Gilbert damping α . Magnetization reversal trajectories of $A_3 = 14 \times 14 \text{ nm}^2$ for damping (b) $\alpha = 0.010$ and (c) $\alpha = 0.017$.

the theoretically calculated frequencies (black line) are plotted in same Figure 5 and noted that the decreasing trends are consistent as expected. Later on, by keeping the minimal $f_0(H_{\text{shape}})$ and optimal $\eta(H_{\text{shape}})$ (i.e., corresponding to different A or H_{shape}) fixed, we investigate the minimally required amplitude H_{mw} (red square) as a function of H_{shape} . Figure 5 shows that H_{mw} also decreases with the increase of H_{shape} . This is explained by the same reason of reducing the height of the energy barrier with H_{shape} as shown in the Figure 2(b). So even the smaller amplitude H_{mw} can drive faster magnetization reversal.

The Gilbert damping coefficient α is an important material parameter which has a significant effect on the magnetization reversal process as well as switching time. In general, damping has two influences. First, it hinders energy absorption (cost more energy) during climbing the energy barrier for magnetization reversal [50]. Second, after crossing the energy barrier, it dissipates the energy of magnetization promptly and thus it accelerates the magnetization to reach the ground/stable state [51, 52]. However, in the magnetization switching process, the magnetization requires to climb an energy barrier (originated from the anisotropy field) and then goes to a stable state. Ideally, for the fast and energy-efficient magnetization reversal, smaller (larger) damping (α) before (after) cross over the energy barrier is better. Therefore, this study emphasizes finding the optimal α of the sample of different A at which the fastest reversal is valid. Accordingly, DCMP-driven magnetization as a function of α for different A is studied. Figure 6(a) shows the Gilbert damping dependence of switching time for different A . It is found that for $A_0 = 8 \times 8 \text{ nm}^2$ (uniaxial sample), the range of α is small but for finite shape anisotropy (biaxial sample), the range of α is large which is useful in device application. Moreover, for the sample of $14 \times 14 \text{ nm}^2$, the switching time is lowest ($t_s = 0.482 \text{ ns}$) at $\alpha = 0.017$. To be more explicit, Figure 6(b) and 6(c) show the trajectories of magnetization reversal for $\alpha = 0.01$ and $\alpha = 0.017$ respectively and observed that for $\alpha = 0.017$, the reversal path is shorter. This is happened because, after cross over the en-

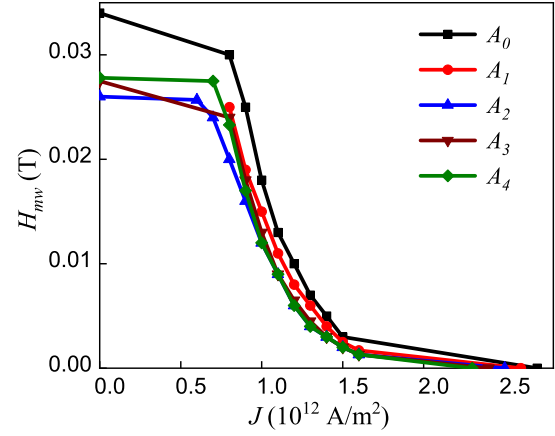


Figure 7: Phase diagram, for magnetization switching within 1 ns, in terms of DCMP field amplitudes H_{mw} and current density J for the samples of different A .

ergy barrier, the larger α reduces the magnetization precession by dissipating the magnetization energy promptly and thus, it leads to fast reversal. It is indicated that there is a specific sample that has an optimal damping situation at which the magnetization reversal might be fastest.

For most device application, the desired microwave pulse (DCMP) should be of smaller amplitude H_{mw} , smaller initial frequency f_o and low chirp rate η , but we have obtained, for a sample of $A = 16 \times 16 \text{ nm}^2$, minimal $H_{\text{mw}} = 0.0278 \text{ T}$, optimum $f_o = 12.4 \text{ GHz}$, and $\eta = 40.672 \text{ ns}^{-2}$. In order to further reduce H_{mw} , we simultaneously apply a direct current such that it assists the magnetization reversal induced by DCMP. For DCMP contribution, we tune H_{mw} while the minimal f_o and optimal η corresponding to different A kept fixed. Figure 7 shows the $H_{\text{mw}} - J$ phase diagram for the sample of different A under the condition of magnetization reversal time 1 ns. As an example, for $A = 16 \times 16 \text{ nm}^2$, without DCMP, the required current to obtain fast switching gets very high i.e., $J = 2.3 \times 10^{12} \text{ A/m}^2$ while without current i.e., $J = 0$, the $H_{\text{mw}} = 0.0278 \text{ T}$ is large from practical point of view. Therefore, with simultaneous applying of DCMP and current, the required values of H_{mw} and J could be smaller than the above mentioned values (for individual case) which gives a large scope of practical realization of this DCMP-driven magnetization reversal strategy.

4. Discussion and Conclusions

This study investigates the influence of shape anisotropy on the DCMP-driven magnetization reversal time t_s and the three controlling parameters (H_{mw} , f_o and η) of DCMP, and damping dependence of magnetization reversal. The shape anisotropy interestingly assists magnetization reversal since the parameters of DCMP H_{mw} , f_o and η decrease with the increase of shape anisotropy H_{shape} . For the sample of $A_8 \geq 32 \times 32 \text{ nm}^2$, t_s significantly reduces to 0.346 ns . The minimal parameters of DCMP are estimated as $H_{\text{mw}} = 0.0187 \text{ T}$, $f_o = 5.2 \text{ GHz}$, and optimal $\eta = 24.96 \text{ ns}^{-2}$ which

are useful in device application. These findings can be attributed to the shape anisotropy H_{shape} which reduces the effective anisotropy and thus reduces the height of the energy barrier. The DCMP stimulates efficient energy absorption and emission during magnetization reversal. A recent study [43] reported that the temperature effect also assists the magnetization reversal, i.e., it reduces the parameters of microwave field pulse. Therefore, it is desired that, at finite temperature, the estimated values of H_{mw} , f_o and η would be decreased further (which is beyond the scope of this study). The result of damping dependence of magnetization reversal indicates that for a specific A or H_{shape} , there exists an optimal damping situation. Moreover, it is also shown that the required microwave field amplitude can be lowered by applying the direct current simultaneously. The usage of an optimum combination of both microwave field pulse and current is suggested to achieve cost efficient and faster switching. So these findings may provide the knowledge to fabricate the shape of a single domain nanoparticle to generate the magnetic data storage device.

5. Acknowledgements

This work was supported by the Ministry of Science and Technology (Grant No. 440 EAS) and the Ministry of Education (BANBEIS, Grant No. SD2019972).

References

- [1] S. Sun, C. B. Murray, D. Weller, L. Folks, A. Moser, Monodisperse FePt nanoparticles and ferromagnetic FePt nanocrystal superlattices, *Science* 287 (5460) (2000) 1989–1992.
- [2] S. Woods, J. Kirtley, S. Sun, R. Koch, Direct investigation of superparamagnetism in Co nanoparticle films, *Physical Review Letters* 87 (13) (2001) 137205.
- [3] D. Zitoun, M. Respaud, M.-C. Fromen, M. J. Casanove, P. Lecante, C. Amiens, B. Chaudret, Magnetic enhancement in nanoscale CoRh particles, *Physical Review Letters* 89 (3) (2002) 037203.
- [4] B. Hillebrands, K. Ounadjela, *Spin dynamics in confined magnetic structures I & II*, Vol. 83, Springer Science & Business Media, 2003.
- [5] S. Mangin, D. Ravelosona, J. Katine, M. Carey, B. Terris, E. E. Fullerton, Current-induced magnetization reversal in nanopillars with perpendicular anisotropy, *Nature materials* 5 (3) (2006) 210–215.
- [6] A. Hubert, R. Schäfer, *Magnetic domains: the analysis of magnetic microstructures* (1998).
- [7] Z. Sun, X. Wang, Fast magnetization switching of stoner particles: A nonlinear dynamics picture, *Physical Review B* 71 (17) (2005) 174430.
- [8] G. Bertotti, C. Serpico, I. D. Mayergoyz, Nonlinear magnetization dynamics under circularly polarized field, *Physical Review Letters* 86 (4) (2001) 724.
- [9] Z. Sun, X. Wang, Strategy to reduce minimal magnetization switching field for stoner particles, *Physical Review B* 73 (9) (2006) 092416.
- [10] S. I. Denisov, T. V. Lyutyy, P. Hänggi, K. N. Trohidou, Dynamical and thermal effects in nanoparticle systems driven by a rotating magnetic field, *Physical Review B* 74 (10) (2006) 104406.
- [11] S. Okamoto, N. Kikuchi, O. Kitakami, Magnetization switching behavior with microwave assistance, *Applied Physics Letters* 93 (10) (2008) 102506.
- [12] J.-G. Zhu, Y. Wang, Microwave assisted magnetic recording utilizing perpendicular spin torque oscillator with switchable perpendicular electrodes, *IEEE Transactions on Magnetics* 46 (3) (2010) 751–757.
- [13] C. Thirion, W. Wernsdorfer, D. Mailly, Switching of magnetization by nonlinear resonance studied in single nanoparticles, *Nature materials* 2 (8) (2003) 524–527.
- [14] K. Rivkin, J. B. Ketterson, Magnetization reversal in the anisotropy-dominated regime using time-dependent magnetic fields, *Applied physics letters* 89 (25) (2006) 252507.
- [15] Z. Wang, M. Wu, Chirped-microwave assisted magnetization reversal, *Journal of Applied Physics* 105 (9) (2009) 093903.
- [16] N. Barros, M. Rassam, H. Jirari, H. Kachkachi, Optimal switching of a nanomagnet assisted by microwaves, *Physical Review B* 83 (14) (2011) 144418.
- [17] N. Barros, H. Rassam, H. Kachkachi, Microwave-assisted switching of a nanomagnet: Analytical determination of the optimal microwave field, *Physical Review B* 88 (1) (2013) 014421.
- [18] T. Tanaka, Y. Otsuka, Y. Furomoto, K. Matsuyama, Y. Nozaki, Selective magnetization switching with microwave assistance for three-dimensional magnetic recording, *Journal of Applied Physics* 113 (14) (2013) 143908.
- [19] G. Klughertz, P.-A. Hervieux, G. Manfredi, Autoresonant control of the magnetization switching in single-domain nanoparticles, *Journal of Physics D: Applied Physics* 47 (34) (2014) 345004.
- [20] J. C. Slonczewski, et al., Current-driven excitation of magnetic multilayers, *Journal of Magnetism and Magnetic Materials* 159 (1) (1996) L1.
- [21] L. Berger, Emission of spin waves by a magnetic multilayer traversed by a current, *Physical Review B* 54 (13) (1996) 9353.
- [22] M. Tsoi, A. Jansen, J. Bass, W.-C. Chiang, M. Seck, V. Tsoi, P. Wyder, Excitation of a magnetic multilayer by an electric current, *Physical Review Letters* 80 (19) (1998) 4281.
- [23] J. A. Katine, F. J. Albert, R. A. Buhrman, E. B. Myers, D. C. Ralph, Current-driven magnetization reversal and spin-wave excitations in Co/Cu/Co pillars, *Phys. Rev. Lett.* 84 (2000) 3149–3152.
- [24] X. Waintal, E. B. Myers, P. W. Brouwer, D. C. Ralph, Role of spin-dependent interface scattering in generating current-induced torques in magnetic multilayers, *Phys. Rev. B* 62 (2000) 12317–12327.
- [25] J. Z. Sun, Spin-current interaction with a monodomain magnetic body: A model study, *Physical Review B* 62 (1) (2000) 570.
- [26] J. Sun, Spintronics gets a magnetic flute, *Nature* 425 (6956) (2003) 359–360.
- [27] M. D. Stiles, A. Zangwill, Anatomy of spin-transfer torque, *Physical Review B* 66 (1) (2002) 014407.
- [28] Y. B. Bazaliy, B. Jones, S.-C. Zhang, Current-induced magnetization switching in small domains of different anisotropies, *Physical Review B* 69 (9) (2004) 094421.
- [29] R. Koch, J. Katine, J. Sun, Time-resolved reversal of spin-transfer switching in a nanomagnet, *Physical Review Letters* 92 (8) (2004) 088302.
- [30] W. Wetzel, G. E. Bauer, O. N. Jouravlev, Efficient magnetization reversal with noisy currents, *Physical review letters* 96 (12) (2006) 127203.
- [31] A. Manchon, S. Zhang, Theory of nonequilibrium intrinsic spin torque in a single nanomagnet, *Physical Review B* 78 (21) (2008) 212405.
- [32] I. M. Miron, G. Gaudin, S. Auffret, B. Rodmacq, A. Schuhl, S. Pizzini, J. Vogel, P. Gambardella, Current-driven spin torque induced by the rashba effect in a ferromagnetic metal layer, *Nature materials* 9 (3) (2010) 230–234.
- [33] I. M. Miron, K. Garello, G. Gaudin, P.-J. Zermatten, M. V. Costache, S. Auffret, S. Bandiera, B. Rodmacq, A. Schuhl, P. Gambardella, Perpendicular switching of a single ferromagnetic layer induced by in-plane current injection, *Nature* 476 (7359) (2011) 189–193.
- [34] L. Liu, C.-F. Pai, Y. Li, H. Tseng, D. Ralph, R. Buhrman, Spin-torque switching with the giant spin hall effect of tantalum, *Science* 336 (6081) (2012) 555–558.
- [35] J. Grollier, V. Cros, H. Jaffres, A. Hamzic, J.-M. George, G. Faini, J. B. Youssef, H. Le Gall, A. Fert, Field dependence of magnetization reversal by spin transfer, *Physical Review B* 67 (17) (2003) 174402.
- [36] H. Morise, S. Nakamura, Stable magnetization states under a spin-polarized current and a magnetic field, *Physical Review B* 71 (1)

- (2005) 014439.
- [37] T. Taniguchi, H. Imamura, Critical current of spin-transfer-torque-driven magnetization dynamics in magnetic multilayers, *Physical Review B* 78 (22) (2008) 224421.
 - [38] Y. Suzuki, A. A. Tulapurkar, C. Chappert, Spin-injection phenomena and applications, in: *Nanomagnetism and Spintronics*, Elsevier, 2009, pp. 93–153.
 - [39] Z. Sun, X. Wang, Theoretical limit of the minimal magnetization switching field and the optimal field pulse for stoner particles, *Physical review letters* 97 (7) (2006) 077205.
 - [40] X. Wang, Z. Sun, Theoretical limit in the magnetization reversal of stoner particles, *Physical Review Letters* 98 (7) (2007) 077201.
 - [41] X. Wang, P. Yan, J. Lu, C. He, Euler equation of the optimal trajectory for the fastest magnetization reversal of nano-magnetic structures, *EPL (Europhysics Letters)* 84 (2) (2008) 27008.
 - [42] M. T. Islam, X. Wang, Y. Zhang, X. Wang, Subnanosecond magnetization reversal of a magnetic nanoparticle driven by a chirp microwave field pulse, *Physical Review B* 97 (22) (2018) 224412.
 - [43] M. Islam, M. Pikul, X. Wang, Thermally assisted magnetization reversal of a magnetic nanoparticle driven by a down-chirp microwave field pulse, *Journal of Magnetism and Magnetic Materials* 537 (2021) 168174.
 - [44] T. Yoo, D. Shin, J. Kim, H. Kim, S. Lee, X. Liu, J. Furdyna, Effect of shape anisotropy on the magnetization reversal process of (ga, mn) as ferromagnetic semiconductors, *Journal of Applied Physics* 103 (7) (2008) 07D119.
 - [45] J. Dubowik, Shape anisotropy of magnetic heterostructures, *Physical Review B* 54 (2) (1996) 1088.
 - [46] R. Skomski, Nanomagnetism, *Journal of Physics: Condensed Matter* 15 (20) (2003) R841.
 - [47] M. Jamet, W. Wernsdorfer, C. Thirion, D. Mailly, V. Dupuis, P. Mélinon, A. Pérez, Magnetic anisotropy of a single cobalt nanocluster, *Physical Review Letters* 86 (20) (2001) 4676.
 - [48] T. L. Gilbert, A phenomenological theory of damping in ferromagnetic materials, *IEEE transactions on magnetics* 40 (6) (2004) 3443–3449.
 - [49] A. Vansteenkiste, J. Leliaert, M. Dvornik, M. Helsen, F. Garcia-Sanchez, B. Van Waeyenberge, The design and verification of mumax3, *AIP Advances* 4 (10) (2014) 107133.
 - [50] Z. Wang, M. Wu, Chirped-microwave assisted magnetization reversal, *Journal of Applied Physics* 105 (9) (2009) 093903.
 - [51] Y. Uesaka, Y. Suzuki, O. Kitakami, Y. Nakatani, N. Hayashi, H. Fukushima, Switching time of a single spin in linearly varying field, *Journal of Applied Physics* 111 (12) (2012) 123907.
 - [52] C. Y. Mao, J.-G. Zhu, R. M. White, T. Min, Effect of damping constant on the switching limit of a thin-film recording head, *Journal of applied physics* 85 (8) (1999) 5870–5872.